Available online at www.sciencedirect.com

SCIENCE DIRECT®

Science of the Total Environment 366 (2006) 837–850

Science of the Total Environment
An International Journal for Scientific Research into the Environment and its Relationship with Humankind

www.elsevier.com/locate/scitotenv

Radionuclide dating (^{210}Pb, ^{137}Cs, ^{241}Am) of recent lake sediments in a highly active geodynamic setting (Lakes Puyehue and Icalma—Chilean Lake District)

F. Arnaud [a,b,1], O. Magand [c,*], E. Chapron [d,2], S. Bertrand [e], X. Boës [e], F. Charlet [d], M.-A. Mélières [c]

[a] *Processus et Bilan en Domaine Sédimentaire, UMR CNRS 8110, Bât. SN5, UST Lille 1, F-59655 Villeneuve d'Ascq, France*
[b] *Géodynamique des Chaînes Alpines, UMR CNRS 5025, Bât. Belledonne, Université de Savoie, F-73373 Le Bourget du Lac, France*
[c] *Laboratoire de Glaciologie et Géophysique de l'Environnement, UMR CNRS 5183, 54 rue Molière, F-38402 Saint Martin d'Hères Cedex, France*
[d] *Renard Centre of Marine Geology, University of Gent, Department of Geology and Soil Science, Krijgslaan 281 S8, B-9000 Gent, Belgium*
[e] *U.R. Argiles et Paléoclimats, University of Liege, Allée du 6 Août, B18, ULG-Sart-Tilman, B-4000 Liège, Belgium*

Received 5 August 2005; accepted 10 August 2005
Available online 22 September 2005

Abstract

This study presents an attempt to use radionuclide profiles to date four short sediment cores taken from two Chilean lakes located in a highly active geodynamic setting. In such settings, sediment series commonly contain earthquake-triggered reworked layers and/or volcanic ash layers. All of these layers affect the vertical distribution of radionuclides. The drawing up of accurate chronologies is made even more problematic by the low fallout rates of both natural (^{210}Pb) and artificial (^{137}Cs, ^{241}Am) radionuclides. However, radionuclide profiles can be "corrected" by subtracting the influence of instantaneous deposits that have been identified from detailed sedimentological studies. Thus, radionuclides can be used to provide approximate dates for sediment. Independent confirmation of these dates can be provided by varve counting and/or the recognition of historical events. For Lake Puyehue, this approach has allowed particular sediment features to be related to the effects of the 1960 Chilean earthquake (Mw 9.5) on the lake basin and its catchment area. For Lake Icalma, there is a good agreement between radionuclide dates and the dates of the three tephra layers formed during large eruptions of the Llaima volcano in 1946, 1917 and 1883. For

* Corresponding author. Tel.: +33 4 76 82 42 59; fax: +33 4 76 82 42 01.
E-mail address: magand@lgge.obs.ujf-grenoble.fr (O. Magand).
[1] Present address: Environnement Dynamique et Territoires de Montagnes, UMR CNRS 5204, Bât. Belledonne, Université de Savoie, F-73373 Le Bourget du Lac, France.
[2] Present address: Geological Institute, ETH Zürich, CH-8092 Zürich, Switzerland. Address to which the proofs should be sent: Olivier Magand, LGGE, UMR CNRS 5183, 54 rue Molière, F-38402 Saint Martin d'Hères Cedex, France.

doi:10.1016/j.scitotenv.2005.08.013

both lakes, artificial radionuclide fallout, which culminated in 1965, provides more robust chronological information than ^{210}Pb dating.

Keywords: ^{210}Pb; ^{137}Cs and ^{241}Am dating; Earthquake; Volcanic eruption; Catastrophic flood; South America; Chile

1. Introduction

Radiometric dating methods have proved their reliability in a large number of studies of lacustrine environments, whether sediment accumulation rates are uniform or non-uniform. When ^{210}Pb and sediment supply mechanisms can be assessed, it is a standard practice to apply one of the three commonly used models: CFCS (Constant Flux, Constant Sedimentation, Goldberg, 1963; Krishnaswami et al., 1971), CRS (Constant Rate of Supply, Appleby and Oldfield, 1983) and CIC (Constant Initial Concentration, Pennington et al., 1976). Whatever the model or procedure used, ^{210}Pb-based chronologies must always be confirmed by independent methods (Smith, 2001). Generally, ^{210}Pb dates are confirmed using ^{137}Cs profiles, when the ^{137}Cs profiles are sufficiently intact (Appleby and Oldfield, 1983). The only source of ^{137}Cs in southern South America is the atmospheric testing of nuclear weapons during the 1950s and 1960s (essentially between 1952 and 1963) (Schuller et al., 1993, 2002). Hence, in the southern hemisphere, ^{137}Cs sediment records can be used to identify sediment layers deposited in 1965 (shortly after most atmospheric testing had ceased) when ^{137}Cs deposition rates were at their peak (Pennington et al., 1973; Cambray et al., 1989; Appleby et al., 1991; UNSCEAR, 2000).

The radionuclide ^{241}Am can be used to corroborate ^{137}Cs dates when the profile has been disturbed. There is a growing evidence that ^{241}Am is less mobile in lake sediments than ^{137}Cs (Appleby et al., 1991) and it is more strongly particle-associated than caesium, especially under low pH conditions (Oldfield et al., 1995). Between 1952 and 1965, direct ^{241}Am fallout was negligible (Krey et al., 1976) and the ^{241}Am found in present-day archives is a decay product of ^{241}Pu from weapons test fallout. Although ^{241}Am activities are much lower than ^{137}Cs activities, Appleby et al. (1991) showed that its distribution in cores is a more accurate marker of maximum fallout (i.e. 1965 in the southern hemisphere) than ^{137}Cs.

In active geodynamic settings, disturbances to radionuclide profiles may preclude the direct use of any ^{210}Pb dating models. Such disturbances can be caused by earthquakes, which rework old ^{210}Pb-depleted material (Arnaud et al., 2002), or by volcanic activity, which leads to the sporadic deposition of variable amounts of volcanoclastic material (e.g. tephra layers). In such cases, artificial radionuclides (^{137}Cs and ^{241}Am) provide indispensable chronostratigraphic markers, but they do not cover the entire 100–150 year span provided by the ^{210}Pb method. When the fingerprints of disturbed sediment layers are well constrained, such sedimentary events may be considered instantaneous deposits that have to be subtracted from the total accumulation in order to assess the mean continuous sedimentation rate (Arnaud et al., 2002; Nomade et al., 2005). Despite these difficulties, the recognition of historical earthquake- or volcanic-triggered deposits in lake sediments may provide additional chronological information that can be used to support data derived from radiometric measurements (Chapron et al., 1999; Ribeiro-Guevara et al., 1999; Arnaud et al., 2002; Nomade et al., 2005).

In this paper, we present the radiometric profiles of four short sediment cores from two lakes in the Chilean Lake District: an area strongly affected by major earthquakes and volcanic eruptions. Our study combined radiometric and sedimentological investigations in order to assess sedimentation rates and the chronological succession of specific layers that may be related to well-documented historical events.

2. Setting

The Chilean Lake District (37° to 42° S, Fig. 1) contains a number of large lakes of glacial origin

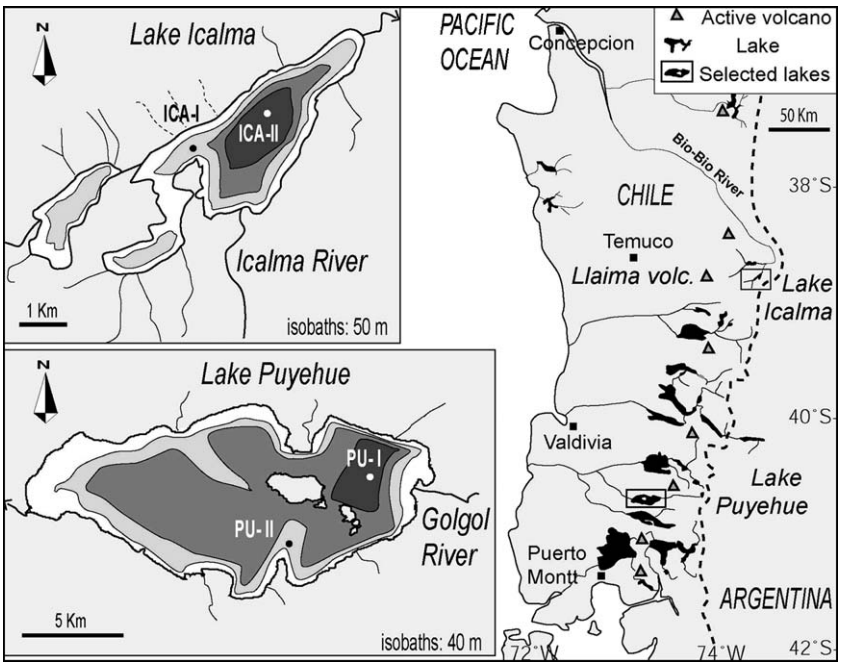

Fig. 1. Location of coring sites in Lakes Icalma and Puyehue within the Chilean Lake District.

(average altitude 700 m). It is a geodynamically active area of the foothills of the Andes Cordillera (which culminates at 3700 m in this region), where the subduction of the Pacific Plate under South America is associated with some of the strongest earthquakes (e.g. the May 1960 Chilean earthquake, Mw 9.5) and some of the most active volcanoes in the Americas (Veyl, 1960; Rothé, 1961; Gerlach et al., 1988; Lara et al., 2004). Sediment cores were taken from Lakes Puyehue (40°40′ S; 72°24′ W) and Icalma (38°50′ S; 71°24′ W). The coring sites were in areas of thick sediment accumulation and limited sediment deformation, as shown by high-resolution seismic reflection mapping (Charlet et al., 2004; Chapron et al., 2004). Lake Puyehue lies in the foothills of the Andes at an altitude of 185 m a.s.l. It covers an area of 165.4 km^2 and has a catchment area of 1267 km^2. It drains the slopes of the Puyehue and Antillanca volcanoes, which are largely composed of Quaternary and Tertiary volcanic rocks covered by comparatively thin andosoils. Most of the catchment area is covered by very dense temperate evergreen rainforest (Veblen and Ashton, 1978; Laugénie, 1982). Lake Icalma lies within the Andes at an altitude of 1150 m a.s.l. It covers an area of 9.8 km^2 and has a catchment area of 148 km^2 characterised by thick soils developed on volcanic ash (i.e. andosoils, Mardones et al., 1993; Veit, 1994).

3. Methods

3.1. Sediment sampling

The UWITEC gravity coring system consists of a 1.2 m transparent plastic liner mounted with an "orange-peel" core catcher. Sampling was carried out in February 2002 to recover 0.5 to 0.6 m-long undisturbed sediment cores from water depths of 122 m (PU-I) and 48 m (PU-II) in Lake Puyehue and 77 m (ICA-I) and 135 m (ICA-II) in Lake Icalma. In each lake, one coring site (PU-I and ICA-II) was selected in a proximal position relative to the main tributary (Rivers Golgol and Icalma, respectively; Fig. 1) and a second site was selected in a more distal part of the lake. The distal site in Lake Puyehue was on a sedimentary ridge covering a subaqueous moraine (PU-II); in Lake Icalma it was in a shallower sub-basin (ICA-II).

After collection, the cores were carefully sealed to preserve the mud-line. They were then transported by

containership to Europe, where they were opened and analysed. For each coring site, the best preserved short core was selected for detailed sediment characterisation and radionuclide dating.

3.2. Sedimentological investigations

One half of the core was used for producing a detailed description of the lithologies and for characterising the sediment (at 0.5 cm intervals) by measuring: (i) grain size, using a Malvern Mastersizer 2000 laser diffraction particle analyser; (ii) gamma density, using a GEOTEK multi sensor track; and (iii) magnetic susceptibility, using a Bartington MS2E1 surface scanning sensor (Bertrand et al., 2005). The uppermost 20 cm of the other half-core was sectioned at 1 cm intervals and samples were stored in plastic bags for radionuclide dating. For both Lake Puyehue coring sites, one half of a twin core was used for the preparation of large format thin sections (Boës et al.,

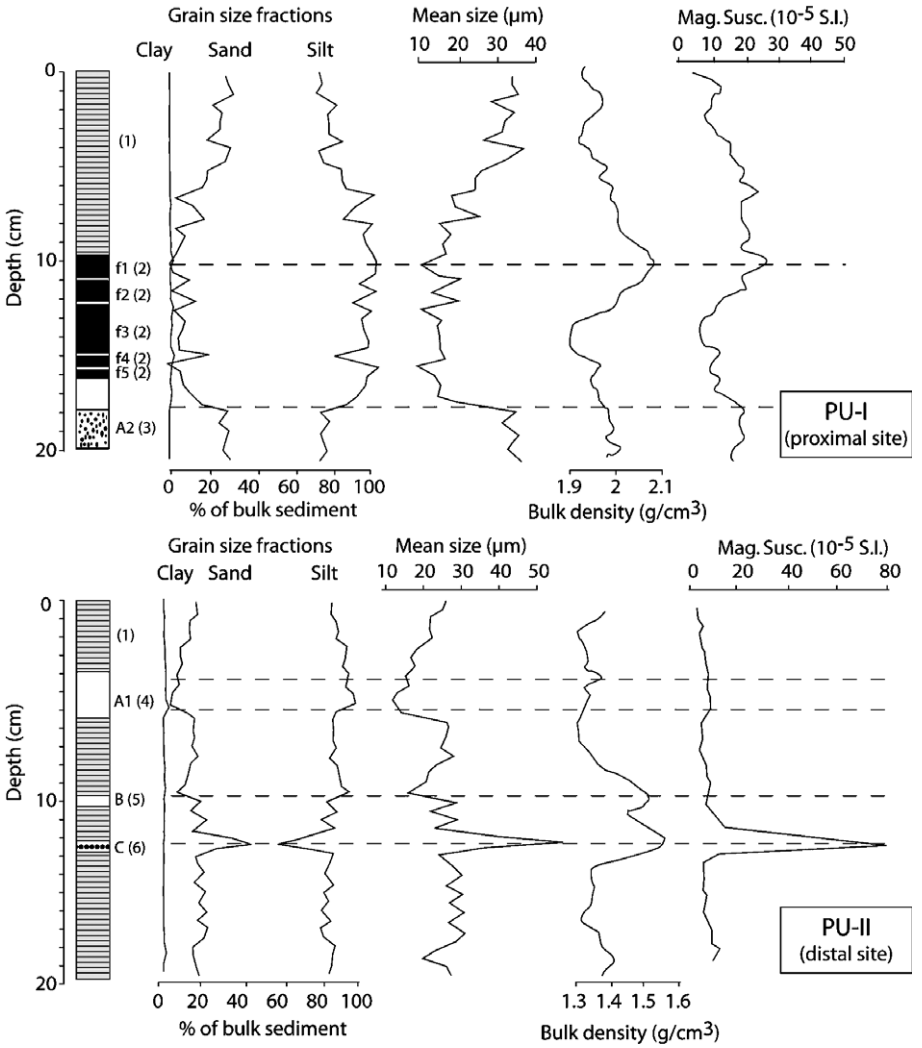

Fig. 2. Detailed sedimentology (facies description, grain size, bulk density, and magnetic susceptibility) of the uppermost 20 cm of Lake Puyehue cores. Key of the sediment logs: (1) background sedimentation: light brown laminated silts; (2) sequence of centimetric (f1, f2 and f3) and milimetric flood deposits (f4 and f5) noted (F); (3) massive silty deposit (A2) (4) sandy silt graded deposit (A1); (5) green lamina (volcanic ash); (6) sandy tephra deposit (1) finely laminated light brown silts.

2004). These thin sections were used to provide a more detailed analysis of the measurements presented in Fig. 2, which are averages taken over several laminae.

3.3. Radiometric measurements

Samples were dried at 60 °C for 3 days, and then weighed to estimate dry bulk density and cumulative mass depth. The dried samples were homogenised with a pestle and mortar before conditioning and analysis (Hernandez, 2002; Hernandez and El-Daoushy, 2002). For Gamma counting, the samples were put into polystyrene tubes. Excess ^{210}Pb (^{210}Pb$_{xs}$) was determined by subtracting the specific activity of ^{214}Pb (i.e. ^{226}Ra) from the total ^{210}Pb specific activity. This calculation is based on the assumption that the intermediate daughter product, ^{222}Rn, is in equilibrium with ^{214}Pb (i.e. ^{226}Ra). The samples were then sealed and left for three weeks to allow equilibrium to be reached before gamma counts were carried out.

Radiometric measurements were performed in a very low background P-type germanium well detector (Canberra Industries), which offers a relative efficiency of 40% and a 4π counting geometry. The counting device was placed in a low-level background laboratory, in order to ensure a very low detection threshold for environmental radioactivity. Such a precaution is particularly necessary for the isotopes of interest here (^{210}Pb, ^{214}Pb, ^{137}Cs and ^{241}Am). Details of the method are given in Pinglot and Pourchet (1994, 1995). This analytical process allowed us to measure ^{137}Cs and ^{210}Pb isotopes with detection limits of below 2 and 10 mBq g^{-1}, respectively. The experimental errors for these measurements, taking into account the different sources of error due to the sampling and analytical procedures, were approximately ±20% for ^{137}Cs and ^{210}Pb, and ±50% for ^{241}Am. Counts were carried out on individual samples for time periods ranging from 10^5 to 3×10^5 s. Every 20 samples, the background level was measured over periods of 2×10^5 to 3×10^5 s.

Sample specific activity A, and total uncertainties of calculated specific activity values, σ_A, are expressed in Becquerel per kilogram of dry weight (Bq kg^{-1} dry wt). The standard deviation expresses the 95% confidence level NRC.

4. Results

4.1. Sedimentology

4.1.1. Lake Puyehue sediments

Lake Puyehue background sediments consist of light-brown, finely laminated sandy silts with very low clay contents. The only variability in mean grain size is due to changes in the relative proportions of sand and silt (Fig. 2). Throughout the cores, sediment grain size, bulk density and magnetic susceptibility measurements showed less variation at the distal coring site (PU-II) than at the proximal site (PU-I). However, both sites provided evidence of sedimentary events that differed markedly from the background sedimentation. These events are characterised by significant changes in grain size, bulk density and magnetic susceptibility (Fig. 2). The thicknesses and compositions of these sedimentary layers were also visible in the thin sections. These layers are clearly different to the background sediment, which consists of couplets of diatom-rich, light-coloured laminae and organic-rich, but slightly clastic, dark-coloured laminae (Boës et al., 2004).

The uppermost 20 cm of the core taken from the proximal site PU-I (Fig. 2—upper panel) includes five fine-silt deposits (labelled f1 to f5, mean size <20 μm) with thicknesses ranging from a few millimetres to 3 cm (f3) and the top of a massive sandy silt deposit (A2). The fine-silt deposits, f1 to f5, have a sharp base and an uneven top—two features that are typical of hyperpycnal flood deposits (Chapron et al., 1999, 2002). These deposits are associated with a fall in bulk density, suggesting high sedimentation rates. Thin section analysis showed that these deposits consist of river-borne material and contain no diatoms. Therefore, the 10 to 18 cm depth portion of core PU-I may be considered a single sedimentary unit of repeated exceptional flood deposits, hereinafter labelled "F". Although its genesis is still open to discussion, the massive sandy silt deposit (A2) is very different to the background sediment and has been interpreted as an "instantaneous deposit". The bottom of this event lies far below the limit of the radionuclide investigation, which focused on the uppermost 20 cm of sediment.

In PU-II (Fig. 2—lower panel), three sedimentary events were recognised in the uppermost 20 cm. A

massive silt layer (A1) of reworked lacustrine sediments was revealed by the impregnated thin sections (Boës et al., 2004) and grain size distribution (Chapron et al., 2004). This is interpreted as a sub-aqueous mass wasting deposit. A layer of silty green sediment (B), which is denser than the host mud, has been attributed to the alteration of a volcanic ash layer (Bertrand et al., 2005). There is also a sandy tephra layer (C), characterised by a peak in density and magnetic susceptibility.

4.1.2. Lake Icalma sediments

Lake Icalma background sediments consist of dark brown sandy silts with mean grain sizes of 40 to 80 μm (Chapron et al., 2004; Bertrand, 2005). Lamination was only observed locally in ICA-I, below a depth of 20 cm (Bertrand, 2005). Specific sedimentary features were recognised by their contrasting lithology (Bertrand, 2005) and grain size (Fig. 3). At both core sites, they consist of successive silty-sand tephra layers, with mean grain sizes of between 150 and 200 μm, and a slump of reworked older sediments.

At both Lake Icalma core sites, several 0.2 to 0.5 cm-thick sandy tephra deposits (a, b, c, d and e) are interbedded with the background sediment. This is also the case for a characteristic yellowish fine-silt layer (f), which was found in the 19–19.5 cm sample from the proximal site (ICA-II, Fig. 3—upper panel) and in the 13.5–14 cm sample from the distal site (ICA-I, Fig. 3—lower panel), as well as in a slump deposit that was seen at a depth of 40 cm in both cores (Bertrand, 2005).

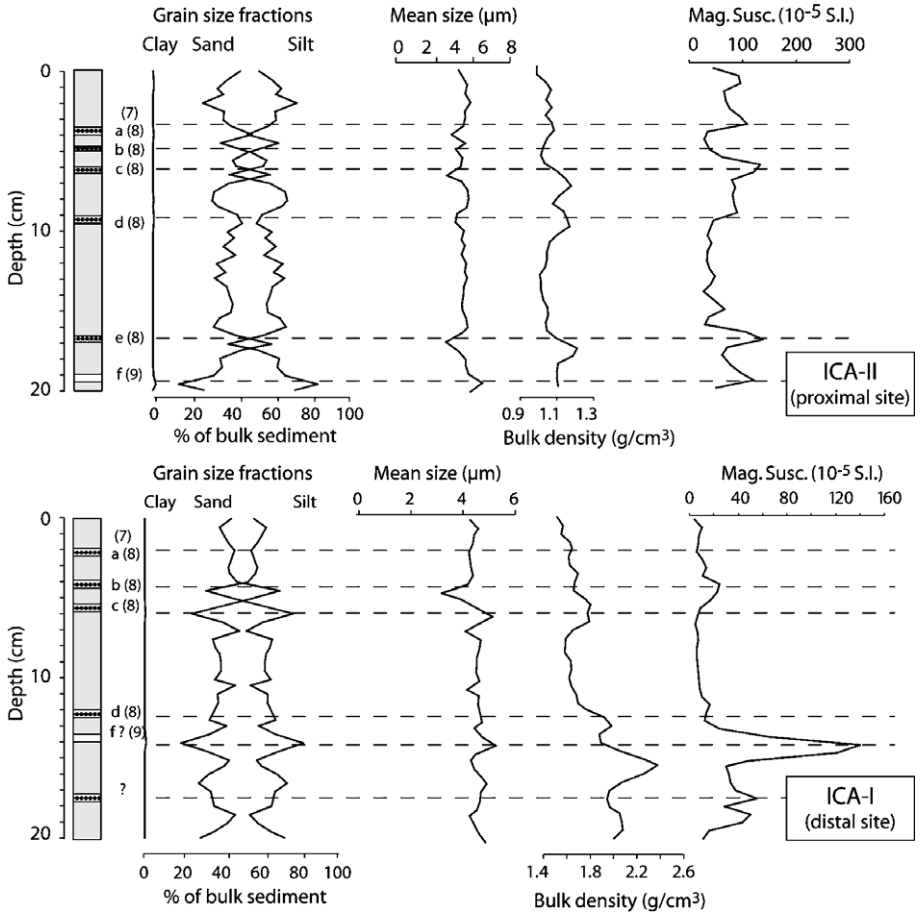

Fig. 3. Detailed sedimentology (facies description, grain size, bulk density, and magnetic susceptibility) of the uppermost 20 cm of Lake Icalma cores. Key of the sediment logs: (7) background sedimentation: dark brown silts; (8) sandy tephra deposits; (9) yellowish fine grained layer.

4.2. Radiometric profiles

4.2.1. Lake Puyehue proximal site (PU-I)

The $^{210}Pb_{xs}$ specific activity profile was relatively homogeneous for depths of between 10 and 19 cm (Fig. 4—upper panel). The ^{137}Cs profile reached a peak at between 4 and 8 cm and then decreased slowly from 6 to 12 cm. Similarly, the underlying samples exhibited homogeneous ^{137}Cs specific activities at depths of between 12 and 20 cm. The depth at which ^{137}Cs is no longer detectable in the sediment profile at this site has not yet been determined. The depths at which radionuclide specific activities are homogenous coincide with the presence of the fine-silt flood deposits (F) and A2 sedimentary events described above. No trace of ^{241}Am was detected in this core.

The results of the sedimentological analysis were used to correct the original radionuclide data for the effect of sedimentary events F and A2 (Arnaud et al., 2002; Nomade et al., 2005). The new profiles (Fig. 4—upper panel, right) show a more continuous decrease in $^{210}Pb_{xs}$ specific activity.

4.2.2. Lake Puyehue distal site (PU-II)

In core PU-II, $^{210}Pb_{xs}$ specific activity decreased continuously along the original profile (Fig. 4—lower

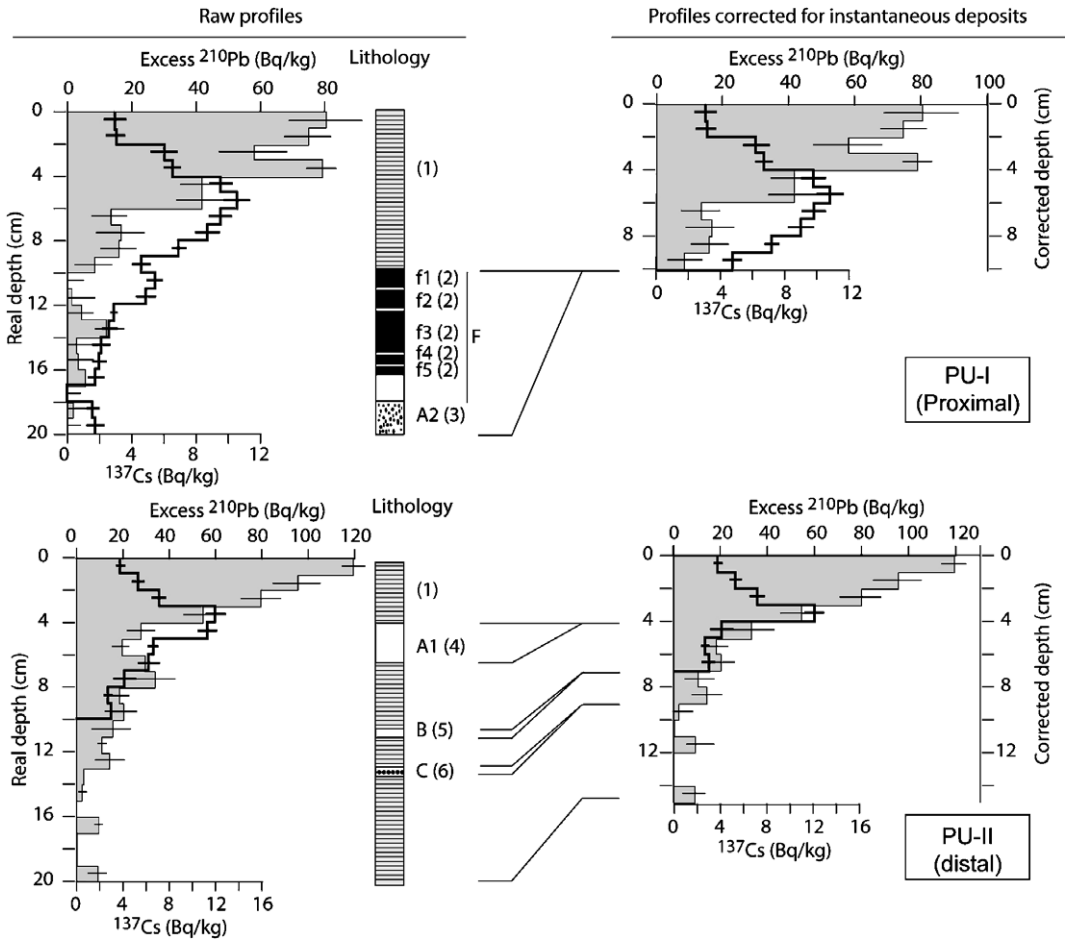

Fig. 4. Radionuclides profiles ($^{210}Pb_{xs}$ and ^{137}Cs) and lithology of lake Puyehue cores. Excess ^{210}Pb (grey area) and ^{137}Cs (bold line) are given in massic activities (Bq kg^{-1} dry weight). Error bars are expressed as 95% confidence level. Left-hand panel shows the original profiles and lithological logs, corrected profiles are plotted on right-hand. They have been computed by substracting the thicknesses of sedimentary events F and A2 in cores PU-I and A1, B and C in PU-II.

panel, left), except between 4 and 6 cm where ^{210}Pb profile is markedly depleted. Radioactive equilibrium was reached at core depth 15–16 cm. Samples at depths of 16–17 cm and 19–20 cm had low $^{210}Pb_{xs}$ specific activities of 10 ± 8 and 9 ± 4 Bq kg^{-1} dry wt, respectively (Fig. 4—lower panel, left). The ^{137}Cs profile is better defined than at the proximal site; the global fallout peak is more pronounced (3–5 cm) and there is no ^{137}Cs specific activity below a depth of 10 cm. Traces of ^{241}Am (0.5 ± 0.3, 2 ± 0.3, 0.6 ± 0.1 Bq kg^{-1} dry wt in samples 3–4, 4–5 and 5–6 cm, respectively) were detected at the same depth as the ^{137}Cs peak which was recognised between 3 and 5 cm.

Because of the three sedimentary events observed in the first 20 cm of the core (events A1, B and C), the original radiometric profiles had to be corrected following the same procedure as for core PU-I. The revised profiles (Fig. 4b—right) no longer show the "depleted" sediment layers with low ^{210}Pb specific activities that were observed in the original samples.

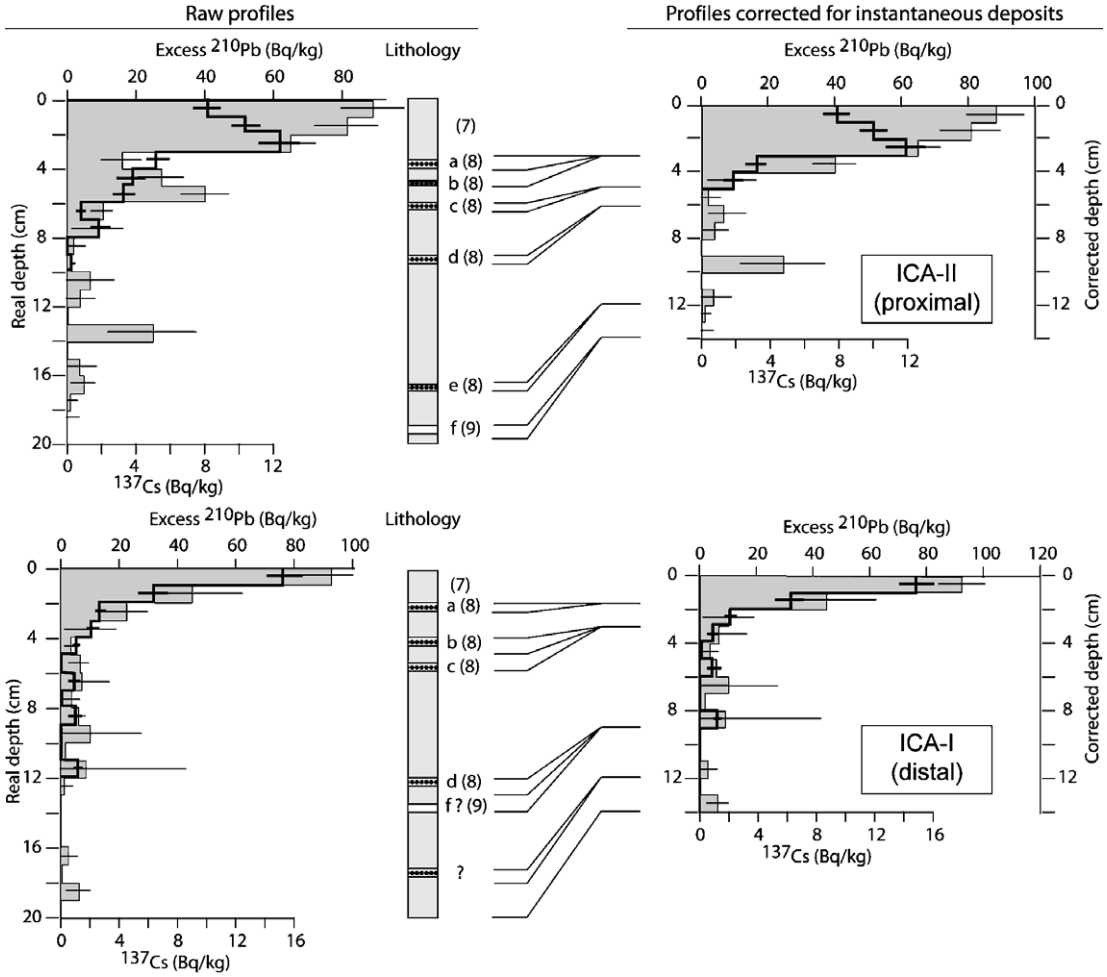

Fig. 5. Radionuclides profiles (^{210}Pbxs and ^{137}Cs) and lithology of lake Icalma cores. Excess ^{210}Pb (grey area) and ^{137}Cs (bold line) are given in massic activities (Bq kg^{-1} dry weight). Error bars are expressed as 95% confidence level. Left-hand panel shows the original profiles and lithological logs, corrected profiles are plotted on right-hand. They have been computed by substracting the thicknesses of sedimentary events a, b, c, d, e and f both in ICA-II and ICA-I.

4.2.3. Lake Icalma proximal site (ICA-II)

The $^{210}Pb_{xs}$ curve for core ICA-II was irregular, with relatively low specific activities between 3 and 5 cm (Fig. 5—upper panel, left). Radioactive equilibrium was reached at a depth of 12–13 cm. Some of the samples from below the apparent equilibrium depth (13–14, 15–16 and 16–17 cm) showed non-zero $^{210}Pb_{xs}$ specific activities (25 ± 13, 4 ± 5, and 5 ± 3 Bq kg^{-1} dry wt, respectively; Fig. 5—upper panel, left). Given the low specific activities and associated high standard deviation, these sample values are not considered representative. For core ICA-II, maximum ^{137}Cs specific activities were obtained at a depth of 2–3 cm; they then decreased rapidly, reaching undetectable levels at a depth of 7–8 cm. ^{241}Am was not detected in any of the samples. The corrected profiles (Fig. 5—upper panel, right) for the upper part of the core (0–10 cm) are significantly less irregular.

4.2.4. Lake Icalma distal site (ICA-I)

In core ICA-I (Fig. 5—lower panel, left), $^{210}Pb_{xs}$ specific activity decreased very rapidly close the surface (0 to 4 cm). Specific activity values for depths of between 4 and 12 cm were relatively homogeneous (between 1 and 10 Bq kg^{-1} dry wt). As previously shown, two of the sediment layers (16–17 and 18–19 cm) below the considered equilibrium depth showed low $^{210}Pb_{xs}$ specific activities.

In contrast to all of the cores described above, the ^{137}Cs profile did not show a peak and ^{137}Cs was concentrated in the first 2 cm. The specific activities detected in subsequent samples (2–5 cm) were below 2 Bq kg^{-1} dry wt, close to detection limit. Traces of ^{137}Cs were also detected at three deeper levels (6–7, 8–9 and 11–12 cm). ^{241}Am was only detected in the uppermost centimetre (1.0 ± 0.5 Bq kg^{-1} dry wt). Moreover, the ^{137}Cs specific activities profile is similar ($r^2 = 0.97$; $n = 8$) to the $^{210}Pb_{xs}$ specific activities profile, both of which show an exponential decay. This is an unexpected result for an artificial radionuclide that was only deposited at certain moments in time. In core ICA-I, the rough similarities in the shapes of both profiles and in the behaviour of ^{137}Cs and ^{210}Pb may suggest a common transfer process within the sediment. Correction of the original data for sedimentary events (Fig. 5—lower panel, right) did not significantly change the profiles.

5. Assessment of age–depth relationships by comparing radionuclide profiles and historical data

The cores from both lakes were first dated using ^{137}Cs, and then by the application of ^{210}Pb-derived models. In each case, the resulting data were compared with independently derived time scales, i.e. varve counting (in Lake Puyehue) and the recognition of sedimentary features triggered by historical geodynamic events. A synthesis of the estimated and calculated ages of the sedimentary events (or instantaneous deposits) in all the cores is presented in Table 1.

5.1. Lake Puyehue

5.1.1. Artificial radionuclides

In core PU-I, traces of ^{137}Cs were found in the lowest sample (Fig. 4—upper panel) and the ^{137}Cs peak at 5–6 cm did not become more pronounced after the results were corrected for sedimentary events below 10 cm. However, the shape of this peak might be due to a change in sedimentation rates in the uppermost 10 cm of the core, as shown by an increase in mean grain size and by slight decreases in bulk density and magnetic susceptibility (Fig. 2—upper panel). Nevertheless, comparisons with previous studies of southern hemisphere sediments (Robbins, 1978; Wise, 1980; Longmore, 1983; Longmore et al., 1983) suggest that the ^{137}Cs peak at 5–6 cm corresponds to maximum bomb test radionuclide fallout in 1965.

This interpretation is supported by core PU-II (Fig. 4—upper panel), in which the ^{137}Cs peak at 3–4 cm is very sharp and associated with traces of ^{241}Am. Thus, for the period 1965–2002, the sedimentation rates for PU-I and PU-II can be calculated at 1.5 ± 0.1 mm y^{-1} (i.e. 42 ± 4 mg dry wt cm^{-2} y^{-1}) and 0.95 ± 0.15 mm y^{-1} (i.e. 28 ± 1 mg dry wt cm^{-2} y^{-1}), respectively.

For Lake Puyehue, the 1965 maximum fallout was also confirmed by varve counting on thin sections from both coring sites. Furthermore, varve counting and sedimentological evidence suggests that the A1 (in the distal site) and A2 (in the proximal site) deposits may be associated with the 1960 Chilean earthquake (Boës et al., 2004; Chapron et al., 2004)—the most powerful earthquake ever recorded on Earth (Veyl, 1960; Rothé, 1961; Gerlach et al.,

Table 1
Synthesis of the calculated and estimated ages of sedimentary events (or instantaneous deposits) in cores PU-I, PU-II, ICA-I and ICA-II

	Calendar years (AD)				
	^{210}Pb CFCS	^{137}Cs	^{241}Am	Varve counting[a]	Historical events
PU-I (near river site)					
F (10–18 cm)[b]	n.a.[c,b]	Older than 1965[b]	n.d.[d]	/	?
A2 (18–30 or 52 cm)	/	/	/	/	1960
PU-II (distal site)					
A1 (4–6.5 cm)	1962 ± 2	1960 ± 6[e]	1960 ± 6[e]	1960	1960
B (10.5–11 cm)	1922 ± 4	/	/	1944	?
C (13–14 cm)	1902 ± 5	/	/	1936	1921
ICA-II (near river site)					
a (3.5–4 cm)	1937 ± 5	1948 ± 6[e]	n.d.[d]	/	1946
b (4.8–5 cm)	1916 ± 2	/	/	/	1917
c (6–6.5 cm)	1892 ± 5	/	/	/	1883
d (9–9.5 cm)	n.a.[c,b]	/	/	/	
e (16.5–17 cm)	n.a.[c,b]	/	/	/	
f (19–19.5 cm)	n.a[c,b]	/	/	/	
ICA-I (distal site)					
a (2–2.5 cm)	1949 ± 3	Below fifties[b]	Below fifties[b]	/	1946
b (4–4.5 cm)	1910 ± 5	/	/	/	1917
c (5–5.5 cm)	1864 ± 6	/	/	/	1883
d (12–12.5 cm)	n.a.[c,b]	/	/	/	?

Comparison between C.F.C.S. age-models, artificial radionuclides (^{137}Cs and ^{241}Am), varve counting and historical events absolute dating.
[a] After Boës et al. 2004.
[b] Cf. discussions in text.
[c] Not applicable.
[d] Not detected.
[e] Extrapolation of ^{137} Cs-derived SR in sample below caesium peak.

1988; Lara et al., 2004). This conclusion is supported by the ^{137}Cs profile for the proximal site (PU-I), in which the ^{137}Cs peak is at 5–6 cm, i.e. above the F deposit. One corollary of this is a very high sedimentation rate (~25 mm y^{-1}) following the 1960 event, which would partly explain the poor peak definition. Such a conclusion also provides confirmation for the interpretation of Chapron et al (2004) of the F deposit as a succession of thick flood deposits related to the reaction of the River Golgol to the numerous landslides that temporarily dammed its course following the 1960 earthquake (Tazieff, 1962; Wright and Mella, 1963; Veblen and Ashton, 1978). The very high sedimentation rate that such a scenario invokes is consistent with the radiometric results.

In core PU-I, the A1 layer lies between the beginning of nuclear testing (1952) and maximum radionuclide fallout (1965), which supports the conclusion that the formation of this layer is related to the 1960 Chilean earthquake. The relative proximity of the 1965 peak and the A1 deposit indicates that this site was not affected by the outburst events that occurred in the Golgol catchment area.

5.1.2. *^{210}Pb-derived dating*

In core PU-I (Figs. 2 and 3), the occurrence of a succession of thick flood deposits and sedimentary events (except A2) indicates a very variable sedimentation rate. Consequently, this deposit does not meet the conditions for applying the so-called Constant Flux, Constant Sedimentation (CFCS) model (Robbins, 1978). As the ^{210}Pb$_{xs}$ profile of the corrected plot is non-linear, it cannot be used to calculate mean sedimentation rates for the past 100–150 years.

An alternative way to analyse such a profile would be to assume that there is a Constant net Rate of

Supply (CRS) of ^{210}Pb from the lake water to the sediment, irrespective of changes that may have occurred in the net dry mass sedimentation rate (Goldberg, 1963; Appleby and Oldfield, 1978; Robbins, 1978). However, application of the CRS model yielded aberrant results (not shown). According to Appleby and Oldfield (1992), the CRS model is unlikely to be valid when the $^{210}Pb_{xs}$ is mostly derived from the catchment area. As the ^{137}Cs data shows, between 1960 and 1965 the PU-I site received a substantial sediment-associated radionuclide input from its catchment area in addition to the direct atmospheric input. These radionuclides came from soils that were destabilised by the huge landslides that occurred during the five years following the 1960 Chilean earthquake. As a result, it is not possible to apply any ^{210}Pb age-model to this core.

In core PU-II (upper panels of Figs. 2 and 4), the $^{210}Pb_{xs}$ corrected profile corresponds to sediments deposited under continuous sedimentation processes, as all the points in this profile were obtained from thin laminae couplets. The conditions required to apply the CFCS age-model are therefore met. The resulting mean sedimentation rate was calculated to be 1.0 ± 0.1 mm y^{-1} ($r^2 = 0.94$) (28 ± 1 mg dry wt cm^{-2} y^{-1}; $r^2 = 0.93$) ($n = 9$), which is similar to the rate obtained from the ^{137}Cs analysis (0.95 ± 0.15 mm y^{-1}). The CFCS ^{210}Pb-derived estimates of PU-II sediment age can also be compared with ages calculated by counting annual laminae. In this core, the validity of the varve counting results was confirmed by the correlation of event A1 with the impact of the 1960 earthquake and by the correlation of the tephra (event C) with the well-documented Puyehue–Cordon–Caulle eruption during the 1921–22 austral summer (Gerlach et al., 1988; Lara et al., 2004). The age/depth curve shows that the CFCS model and the annual varve counting ages differ by less than 5 years over the last 40 years (from 1960 to the present day). Below sediment feature A1, the ages estimated by the two methods differ by more than 20 years. This disagreement may be explained by a variation in ^{210}Pb fluxes and/or changes in the rate of supply. Such changes may reflect the intensive logging and agricultural activity in lower areas (<600 m a.s.l.) of the Golgol Valley between 1900 and the 1950s, reported by Wright and Mella (1963) and by Veblen and Ashton (1978).

5.2. Lake Icalma

5.2.1. Artificial radionuclides

In core ICA-II (Fig. 5—upper panel), the maximum ^{137}Cs specific activity measured at 2–3 cm can be interpreted as corresponding to the 1965 fallout. A sedimentation rate of between 0.5 and 0.8 mm y^{-1} (i.e. 17 ± 3 mg dry wt cm^{-2} y^{-1}) can therefore be estimated for the 1965–2002 period.

In core ICA-I (Fig. 5—lower panel), the ^{137}Cs profile suggests redistribution of the radioisotope within the sediment column due to remobilization processes. This profile also suggests a low accumulation rate. Indeed, ^{241}Am is only detected in the uppermost portion (0–1 cm), which must contain the 1965 reference level. A sedimentation rate of less than 0.3 mm y^{-1} (i.e.<6 mg dry wt cm^{-2} y^{-1}) after 1965 may therefore be deduced.

The down-core extrapolation of these sedimentation rates indicates that the near-surface tephra layer (event "a", at 3–3.5 cm depth in ICA-II and at 2–2.5 cm depth in ICA-I, Fig. 3) marks the last historical eruption of the nearby Llaima stratovolcano in 1946 (Gonzáles-Ferrán, 1994).

5.2.2. ^{210}Pb-derived dating

Since grain size measurements and lithological descriptions suggest quite stable sedimentation conditions for the background sediment at both Lake Icalma core sites (Bertrand, 2005), we applied the CFCS model to estimate their mean sedimentation rates.

For core ICA-II, despite the high standard deviation of the $^{210}Pb_{xs}$ values (Fig. 5—upper panel, right), we estimated a mean sedimentation rate of 0.6 ± 0.1 mm y^{-1} ($r^2 = 0.81$), i.e.: 17 ± 1 mg dry wt cm^{-2} y^{-1} ($r^2 = 0.78$) ($n = 8$), which is in agreement with ^{137}Cs data. This mean sedimentation rate is supported by the correlation of tephra deposits a, b and c with the historical eruptions of the Llaima volcano (Fig. 1) in 1946 (event "a" dated 1937 ± 5 years), 1917 (event "b" dated 1916 ± 2 years) and 1883 (event "c" dated 1892 ± 5 years) (Gonzáles-Ferrán, 1994). There are several historical events that may be responsible for layers "d", "e" and "f", but as they are more than 150 years old, and therefore beyond the range of the ^{210}Pb method, it is not possible to continue the chronology further.

For core ICA-I (Fig. 5—lower panel), the CFCS model gives a mean sedimentation rate of 0.4 ± 0.1 mm y^{-1}, i.e. 12 ± 1 mg dry wt cm^{-2} y^{-1} ($r^2 = 0.99$, $n = 5$). This estimated accumulation rate is slightly different from the value derived from ^{137}Cs data (less than 0.3 mm y^{-1}). It must be remembered that the sedimentation rate for the last 40 years, measured using the ^{137}Cs method, and the rate for the last 100–150 years, measured using the ^{210}Pb model, will not necessarily be the same. By applying a mean sedimentation rate of 0.4 mm y^{-1}, the estimated ages of tephra layers "a" (2–2.5 cm), "b" (4–4.5 cm) and "c" (5–5.5 cm) are 1949 ± 3, 1910 ± 5 and 1864 ± 6 years, respectively. These tephra deposits can reasonably be correlated to the historical eruptions of the Llaima volcano (Fig. 1) in 1946, 1917 and 1883, respectively (Gonzáles-Ferrán, 1994).

6. Conclusion

Our study shows that the application of radiochronological methods in southern Chile is complicated by the highly active geodynamic setting and by the very low rates of artificial and natural fallout. Of the four cores studied, three could be dated using the ^{210}Pb method. None of them presented a well-defined ^{137}Cs peak, although this method gave chronological information for all the cores. ^{241}Am was only detected in the distal core from each lake, where the clastic flux, and thus sedimentation rate, was lower. In each case, the position of the ^{241}Am peak confirms the development of a ^{137}Cs peak in 1965 in these mid-latitudes of the southern hemisphere.

Combining radionuclide dating methods with detailed sedimentological investigations allows sedimentary events to be correlated with well-documented earthquakes or volcanic eruptions.

In Lake Puyehue, our age–depth model for the distal coring site is better constrained, as it is supported by varve counting and the recognition of the impact of the massive 1960 Chilean earthquake. In Lake Icalma, the age–depth relationship is better constrained in the proximal coring site, where the results are supported by the correlation of tephra layers with the well-documented eruptions of Llaima volcano in 1946, 1917 and 1883. Our results confirm the difficulties in using ^{210}Pb data as a geochronological tool. This is true for exponential distributions and even more so when non-exponential profiles are encountered. The interpretation of such profiles must be undertaken with caution. The characteristics of the environment being studied must be taken into account, especially when the geodynamic setting is highly active. In the case described here, the cross-checking of radiometric and sedimentological methods made it possible to better understand and judiciously interpret the radionuclide profiles.

Acknowledgements

The French ministry of research is acknowledged for financial support and ACI Climate Change for funding the analytical equipment of the LGGE underground laboratory. Field work in Chile was made possible through the SSTC project EV/12/10B led by Drs. M. De Batist, N. Fagel and A. Berger. We are particularly grateful to Roberto Urrutia (centro EULA, Concepcion) for helpful logistic support. Waldo San Martin and Alejandro Peña (centro EULA, Concepcion) as well as Pr. Christian Beck and Dr. Vincent Lignier are gratefully acknowledged for the strenuous work they carried out during the coring survey. We thank Dr. James Etienne (ETH Zurich) and Mr. Paul Henderson for their contribution to the improvement of English language.

References

Appleby PG, Oldfield F. The calculation of lead-210 dates assuming a constant rate of supply of unsupported ^{210}Pb to the sediments. Catena 1978;5:1–8.

Appleby PG, Oldfield F. The assessment of ^{210}Pb dates from sites with varying sediment accumulation rates. Hydrobiologia 1983;103:29–35.

Appleby PG, Richardson N, Nolan PJ. ^{241}Am dating of lake sediments. Hydrobiologia 1991;214:35–42.

Appleby PG, Oldfield F. In: Ivanovich M, Haiman RS, editors. Application of lead-210 to sedimentation studies. Oxford: Uranium series disequilibrium; 1992. Chap. 21.

Arnaud F, Lignier V, Revel M, Desmet M, Beck C, Pourchet M, et al. Flood and earthquake disturbance of ^{210}Pb geochronology (Lake Anterne, North French Alps). Terra Nova 2002;14–4:225–32.

Bertrand S, Castiaux J, Boës X, Charlet F, Urrutia R, Espinoza C, et al. Temporal evolution of sediment supply in Puyehue Lake (southern Chile) during the last 600 years: climatic significance. Quat Res 2005;64:163–75.

Bertrand S. Sédimentation lacustre postérieure au dernier maximum glaciaire dans les lacs Icalma et Puyehue (Chili méridional): reconstitution de la variabilité climatique et des événements sismo-tectoniques. Unpublished PhD thesis, Université de Liège 2005. 280 pp. [http://www.epoc.u-bordeaux.fr/ASF/theses/BERTRAND_2005.pdf].

Boës X, Arnaud F, Fagel N. The Varve Record of Puyehue Lake (Meridional Chile), AD 1412-2002. AGU, Fall meeting, 13–17 December 2004, San Fransisco, United States; 2004.

Cambray RS, Playford K, Lewis GNJ, Carpenter RC. Radioactive fallout in air and rain: results to the end of 1987 AERE-R 13226. London: HMSO; 1989.

Chapron E, Beck C, Pourchet M, Deconinck JF. 1822 earthquake-triggered homogenite in Lake Le Bourget (NW Alps). Terra Nova 1999;11:86–92.

Chapron E, Desmet M, De Putter T, Loutre MF, Beck C, Deconinck JF. Climatic variability in the northwestern Alps, France, as evidenced by 600 years of terrigenous sedimentation in Lake Le Bourget. The Holocene 2002;12:177–85.

Chapron E, Bertrand S, Charlet F, Boës X, De Batist M, Fagel N, et al. Sedimentary processes in Lake Puyehue over the last 500 years: implications for paleoenvironmental reconstructions in the Chilean lake district (41° S). Bolletino di Geofisica Teorica ed Applicata 2004;45:238–42.

Charlet F, Marchand C, Bertrand S, Chapron E, Pino M, Urrutia R, et al. Geophysical reconstruction of the sedimentary infill of Lago Icalma (39° S, Chilean lake district) since the last deglaciation. Bolletino di Geofisica Teorica ed Applicata 2004;45:179–84.

Gerlach DC, Frey F, Moreno H, López-E L. Recent volcanism in the Puyehue–Cordón Caulle region, southern Andes, Chile (405° S): petrogenesis of evolved lavas. J Petrol 1988;29:333–82.

Goldberg ED. Geochronology with ^{210}Pb: radioactive dating. Vienna, Austria: International Atomic Energy Agency; 1963.

Gonzáles-Ferrán O. Volcanes de Chile. Instituto geográfico militar; 1994. 635 pp.

Hernandez Suarez FJ. Optimisation of Environmental Gamma Spectrometry using Monte-Carlo methods. In: Thesis, Acta Universitatis Upsaliensis, Uppsala; 2002:751. 63 pp.

Hernandez Suarez FJ, El-Daoushy F. Semi-empirical method for the self-absorption correction of photons with energies as low as 10 Kev in environmental samples. Nucl Instrum Methods Phys Res A 2002;484:625–41.

Krey PW, Hardy EP, Pachuki C, Rourke F, Coluzza J, Benson WK. Mass isotopic composition of global fall-out plutonium in soil. Proceedings of the conference on transuranium nuclides in the environment. Vienna, Austria: IAEA; 1976. p. 671–7.

Krishnaswami D, Lal JM, Martin M, Meybeck M. Geochronology of lake sediments. Earth Planet Sci Lett 1971;11:407–14.

Lara LE, Naranjo JA, Moreno H. Rhyodatic fissure eruption in southern Andes (Cordon Caulle, 405° S) after the 1960 (Mw: 95) Chilean earthquake: a structural interpretation. J Volcanol Geotherm Res 2004;138:127–38.

Laugénie C. La région des lacs, Chili méridional. Thèse de doctorat d'état, Université de Bordeaux III; 1982. 822 pp.

Longmore ME. The caesium-137 dating techniques and associated applications in Australia — a review. In: Ambrose W, Duerden P, editors. Archaeometry: an Australian perspective. Canberra, Australia: Aust. Natl. Univ. Press; 1983. p. 310–21.

Longmore ME, O'Leary BM, Rose CW. Caesium-137 profiles in the sediments of a partial meromictic lake on Great Sandy Island (Fraser Island), Queensland, Australia. Hydrobiologia 1983;103:21–7.

Mardones M, Urgate E, Rondanelli M, Rodriguez A, Barrientos C. Planificacion ecologica en el sector Icalma-Liucura (IX region): proposicion de un metodo. Universidad de Concepcion, Monografias Cientificas de EULA; 1993:6. 91 pp.

Nomade J, Chapron E, Desmet M, Reyss L, Arnaud F, Lignier V. Reconstructing historical seismicity from lake sediments (Lake Laffrey, Western Alps, France). Terra Nova 2005;17:350–7.

Oldfield F, Richardson N, Appleby PG. Radiometric dating (^{210}Pb, ^{137}Cs, ^{241}Am) of recent ombrotrophic peat accumulation and evidence for changes in mass balance. The Holocene 1995;5:141–8.

Pennington W, Cambray RS, Fisher EMR. Observations on lake sediments using fallout ^{137}Cs as a tracer. Nature 1973;242:324–6.

Pennington W, Cambray RS, Eakins JD, Harkness DD. Radionuclide dating of the recent sediments of Blelham Tarn. Freshw Biol 1976;6:317–31.

Pinglot JF, Pourchet M. Spectrométrie Gamma à très bas niveau avec Anti-compton NaI (T1) pour l'étude des glaciers et des sédiments. In: CEA-DAMRI, Note CEA N 2756 ISSN 0429-3460. Journées de spectrométrie Gamma et X93, 12-14 Octobre 1993, Paris, France, 1994. 296 pp.

Pinglot JF, Pourchet M. Radioactivity measurements applied to glaciers and lake sediments. Sci Total Environ 1995;173–174:211–23.

Ribeiro-Guevara S, Arribére M, Masaferro J, Villarosa G, Kestelman A. Lead-210 dating of lake sediment cores by using high resolution gamma-ray spctrometry. II South American Symposium on Isotope Geology Cordoba, September 1999. Proceedings; 1999. p. 6–10.

Robbins JA. Geochemical and geophysical applications of radioactive lead isotopes. In: Nriago JP, editor. Biogeochemistry of lead. North Holland: Elsevier; 1978. p. 285–393.

Rothé JP. Les séismes du Chili (21 Mai–21 Juin 1960). Revue pour l'Etude des Calamités 1961;37:3–15.

Schuller P, Lovengreen Ch, Handl J. ^{137}Cs concentration in soil, prairie plants, and milk from sites in southern Chile. Health Phys 1993;64:157–61.

Schuller P, Voigt G, Handl J, Ellies A, Oliva L. Global weapons' fallout ^{137}Cs, in soils and transfer to vegetation in South-Central Chile. J Environ Radioact 2002;62:181–93.

Smith JT. Why should we believe ^{210}Pb sediment geochronologies ? J Environ Radioact 2001;55:121–3.

Tazieff H. Quand la Terre Tremble. Fayard; 1962. 251 pp.

UNSCEAR. Sources and effects of ionizing radiation. UNSCEAR 2000 report to the General Assembly, with scientific annexes. Sources. New York, United Nations; 2000:1. 654 pp.

Veyl OC. Los fenomenos volcanicos y sismicos de fines de mayo de 1960 en el sur de Chile. Universidad de Concepcion, Departemento de Geologia y Mineralogia; 1960. 42 pp.

Veit H. Estratigrafia de capas sedimentarias y suelos correspondientes en el centro-sur de Chile. Rev Chil Hist Nat 1994; 67:395–403.

Veblen TT, Ashton DH. Catastrophic influences on the vegetation of the Valdivian Andes. Chile Vegetario 1978;36:149–67.

Wise SM. Caesium-137 and lead-210: a review of techniques and some applications in geomorphology. In: Cullingford RA, Davidson DA, lewin J, editors. Timescales in geomorphology. London: John Wiley and Sons; 1980. p. 109–27.

Wright C, Mella A. Modifications to the soil pattern of South-Central Chile resulting from seismic and associated phenomena during the period May to August 1960. Bull Seismol Soc Am; 1963. p. 1367–1402.